^{30}Si$(p,\alpha)^{27}$Al reaction from $E_p = 4.90 - 6.08$ MeV

J. S. Chang
Department of Physics, National Taiwan Normal University, Taipei, Republic of China

V. K. C. Cheng and H. H. Lin
Institute of Nuclear Energy Research, Longtan, Taiwan, Republic of China

C. C. Hsu
Department of Physics, National Tsinghua University, Hsinchu, Taiwan, Republic of China

(Received 27 May 1981; revised manuscript received 27 October 1981)

Excitation energies and strengths of sixty-eight resonances in the compound nucleus ^{31}P formed by the reaction ^{30}Si$(p,\alpha)^{27}$Al were observed in the energy range $E_p = 4.90 - 6.08$ MeV. The natural widths of eighteen resonances are reported. The observed level density has been found in good agreement with a semiempirical theory. Angular distributions of ground-state alpha particles, measured at nine resonances, suggested spin and parity for eight levels and level-interference effect for one level.

[NUCLEAR REACTIONS ^{30}Si(p,α), $E = 4.90 - 6.08$ MeV; measured $\sigma(E;E_\alpha,\theta)$, ^{31}P; deduced levels, J, π, orbital momentum mixing ratios; enriched target.]

I. INTRODUCTION

Particle reactions, leading to compound nuclear states, have been proven to be a useful tool for obtaining information on formation parameters, spins, and parities of these resonance states. Resonance states of ^{31}P have been investigated through the reactions of ^{30}Si$(p,\gamma)^{31}$P,[1-6] ^{27}Al$(\alpha,\gamma)^{31}$P,[7] ^{30}Si$(p,p)^{30}$Si,[8-11] and ^{27}Al$(\alpha,p)^{30}$Si.[12] The excitation energy ranges covered by these works were up to about 12.5 MeV. The present work extends information on the resonances in ^{31}P up to the excitation energy 13.2 MeV by the investigation of the ^{30}Si$(p,\alpha)^{27}$Al reaction. The excitation function for the α_0 group has been measured in 2 or 4 keV steps from $E_p = 4.900$ to $E_p = 6.082$ MeV. At least sixty-eight resonances were observed. Their excitation energies, widths, and strengths were determined. The observed level density is compared with theoretical predictions. Angular distributions were also measured at nine resonances of which eight showed forward-backward symmetry and have been analyzed to determine possible spins and parities.

II. EXPERIMENT

Protons from the INER 7 MV Van de Graaff accelerator bombarded an enriched ^{30}Si target situated at the center of a 55 cm diameter scattering chamber. Silicon-30 targets were made by vacuum evaporation of SiO_2 powder, with 98.5% enrichment in ^{30}Si isotope, onto carbon backings of 25 μg/cm^2 thickness. Targets of 42 μg/cm^2 SiO_2 thickness were used throughout the experiment.

For the detection of alpha particles, a detector telescope, composed of a 10 μm thick silicon surface barrier ΔE detector and a 500 μm thick silicon surface barrier E detector, was used. A second 500 μm thick silicon surface barrier detector, fixed at 40° laboratory angle, was used as monitor. Signals from all three detectors were simultaneously analyzed by an ORTEC 6260 computer-based multichannel analyzer system. An electronics block diagram for this experiment is shown in Fig. 1. Beam current was kept at about 300 nA and the deadtimes were negligibly small for all three detectors.

For the excitation function measurement, the

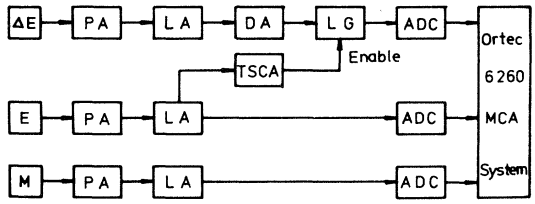

FIG. 1. Electronics block diagram for the ^{30}Si$(p,\alpha)^{27}$Al reaction. PA=preamplifier, LA=linear amplifier, DA=delay amplifier, TSCA=timing single-channel analyzer, LG=linear gate, ADC=analog-to-digital converter.

detector telescope was positioned at 120° laboratory angle and subtended a solid angle of 1.3 msr with respect to the target. While low energy alpha particles produced in the ^{30}Si$(p,\alpha)^{27}$Al reaction ($Q=-2.373$ MeV) are stopped in the ΔE detector, high-energy scattered protons penetrated the ΔE detector and stopped in the E detector. Signals from the E detector were then used to inhibit in a linear gate the overwhelming low energy signals and their pileup pulses in the ΔE detector produced by scattered protons. As a result, the detection resolution is improved and background counts are greatly reduced for the relatively very scarce alpha particles. An excitation function from 4.900 to 6.082 MeV in 2 or 4 keV steps was obtained in this way in a single continuous run.

For the measurement of angular distributions at resonance energies, the detector telescope subtended a solid angle of 0.32 msr. At backward angles data were taken in the same way as in the excitation function measurement. At forward angles, when the energies of all alpha particles were high enough to penetrate through the ΔE detector, the linear gate was operated in normal mode in which the signals from the E detector opened the gate instead. For intermediate angles where alpha energies had stopping ranges approximately equal to the ΔE-detector thickness, spectra in both inhibit and normal modes were accumulated to obtain the total alpha particle yield. Laboratory angles from 30° to 150° have been covered in 10° steps.

The energy calibration of the Van de Graaff accelerator was performed with the threshold reaction ^{7}Li$(p,n)^{7}$Be. The accelerator beam energy resolution was determined to be about ± 1 keV. The beam energy loss at 5 MeV proton energy in the target of SiO_2 was calculated to be 2.6 keV using the tables of Northcliff and Schilling.[13] This leads to a total energy resolution of ± 1.7 keV. On the other hand, the average level spacing in the excitation energy region of this work is estimated from the data of Kuperus[12] to be about 10 keV. Therefore the energy steps in the excitation function measurement, chosen to be 2 keV on the resonance or 4 keV off the resonance, were sufficient to observe and resolve most of the resonances.

III. ANALYSIS

The method of determining resonance strengths, lower limits for particle widths, reduced dimensionless widths, spins, and parities follows the approach of Kuperus *et al.*[12,14–16]

The ratio of the total integrated yields, Y, from two resonances is[17,18]

$$\frac{Y_1}{Y_2}=\frac{E_2}{E_1}\frac{\epsilon_2}{\epsilon_1}\frac{(\omega\gamma)_1}{(\omega\gamma)_2},$$

where E_1 and E_2 are the laboratory bombarding energies of the two resonances, respectively, and $\omega\gamma$ is the resonance strength defined as

$$\omega\gamma=(2J+1)\frac{\Gamma_p\Gamma_\alpha}{\Gamma},$$

where J is the resonance spin, Γ_p is the partial width for the decay of the resonance state by reemission of the bombarding proton, Γ_α is the partial width for the emission of the alpha particle, and Γ is the total width. It is evident that if the resonance strength and the integrated yield are known for one resonance, then a normalization factor can be obtained, and strengths for all other resonances can be determined by taking the ratio of their areas under the excitation curve to the area of the resonance with the known strength.

In the present ^{30}Si$(p,\alpha)^{27}$Al reaction, the total width is approximately the proton width. That is, $\Gamma\simeq\Gamma_p$. Hence $\omega\gamma\simeq(2J+1)\Gamma_\alpha$, which leads to an estimate (or lower limit) for the partial width Γ_α when the resonance spin J is known. Furthermore, when the penetration factor, calculated for the lowest allowed orbital angular momentum in the α decay of a resonance, is divided out from the partial width Γ_α, the reduced alpha-particle width for the resonance level is obtained. A corresponding dimensionless reduced width θ_α^2 is calculated using the expression $\hbar^2/\mu R^2$ for the Wigner limit, μ being the reduced mass and $R=1.4(A_1^{1/3}+A_2^{1/3})$ fm being the nuclear interaction radius of the outgoing system.

In the reaction ^{30}Si$(p,\alpha_0)^{27}$Al [corresponding to

the inverse reaction of the ^{27}Al$(\alpha,p_0)^{30}$Si studied by Kuperus[12]], the spin of the outgoing alpha channel amounts to $\frac{5}{2}$. Thus for most resonances a mixing of three orbital momenta is allowed. For the exit energies discussed here, however, the penetrability for alpha particles with the highest allowed orbital momentum is about one percent of that for alpha particles with the lowest allowed orbital momentum. For this reason only the two lowest orbital momenta of the outgoing alpha particles were considered. There is no orbital momentum mixing in the incident proton channel. The expected angular distribution at a certain isolated resonance, having spin and parity J^π and which can decay with alpha-particle orbital momenta l_α and $l_{\alpha'}$, is then given by

$$W(\theta)=\frac{W(J^\pi,l_\alpha,l_\alpha,\theta)+\varepsilon^2 W(J^\pi,l_{\alpha'},l_{\alpha'},\theta)+2\varepsilon\cos\phi_{l_\alpha l_{\alpha'}} W(J^\pi,l_\alpha,l_{\alpha'},\theta)}{(1+\varepsilon^2)}.$$

In this formula ε is the amplitude ratio and $\phi_{l_\alpha l_{\alpha'}}$ the Coulomb phase difference of the two possible orbital momenta. Theoretical angular distributions $W(J^\pi,l_\alpha,l_{\alpha'},\theta)$ can be calculated using the Legendre polynomial coefficients given in Table I of Kuperus.[12]

After background subtraction, the observed angular distribution was converted to the center-of-mass system. These data were then fitted to the possible one-parameter curves for each value of J^π up to $\frac{17}{2}^+$, determining the value of ε with minimum χ^2 below the 0.1% probability limit. In this way, the possible values of J^π and the corresponding values of ε, as well as the Legendre polynomial coefficients of the angular distribution, could be determined for isolated resonances. The least-square fits were done with a computer program based on the routine CURFIT of Bevington.[19]

IV. RESULTS OF EXPERIMENT AND ANALYSIS

A gated alpha-particle spectrum taken at $\theta_{\rm lab}=120°$ and $E_p=5.695$ MeV is shown in Fig. 2. It is noted that only ground state alpha particles from the ^{30}Si$(p,\alpha)^{27}$Al reaction are observed. This is also true in all the spectra accumulated throughout this work. The absence of the α_1 group, decaying to the first-excited state of ^{27}Al ($E_x=0.844$ MeV, $J^\pi=\frac{1}{2}^+$), may be explained by its much smaller penetrability due to less energy available below the Coulomb barrier. The penetrability is reduced further for α_1 decay from resonances of $J\geq\frac{5}{2}$, because the lowest allowed orbital momentum is two unit higher for α_1 decay than that for α_0 decay.

The yield curve for the α_0 group in the $E_p=4.900-6.082$ MeV region, recorded with the detector telescope at the laboratory angle 120°, is shown in Fig. 3. At least sixty-eight resonances were observed. Table I presents the bombarding energies, excitation energies, and widths, as well as yields and resonance strengths for the α_0 group. All energies in Table I have an error of less than ± 2 keV.

Yields in Table I have been obtained by the integration of the 120° yield curve under the resonance peak. The angular distribution effect has been corrected for when it is known. Resonance strength for the $E_p=5.204$ MeV level was taken from Kuperus's work[12] and used as a normalization to calculate other resonance strengths from their respective integrated yields.

Angular distributions have been measured at nine resonances at $E_p=5.204$, 5.324, 5.512, 5.526, 5.695, 5.720, 5.998, 6.006, and 6.020 MeV. They are sufficiently isolated to try a single-level analysis. Forward-backward symmetry was found

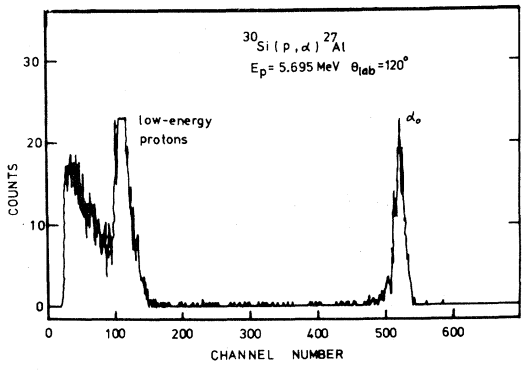

FIG. 2. Gated alpha-particle pulse-height spectrum measured at $\theta_{\rm lab}=120°$ and $E_p=5.695$ MeV for the ^{30}Si$(p,\alpha)^{27}$Al reaction.

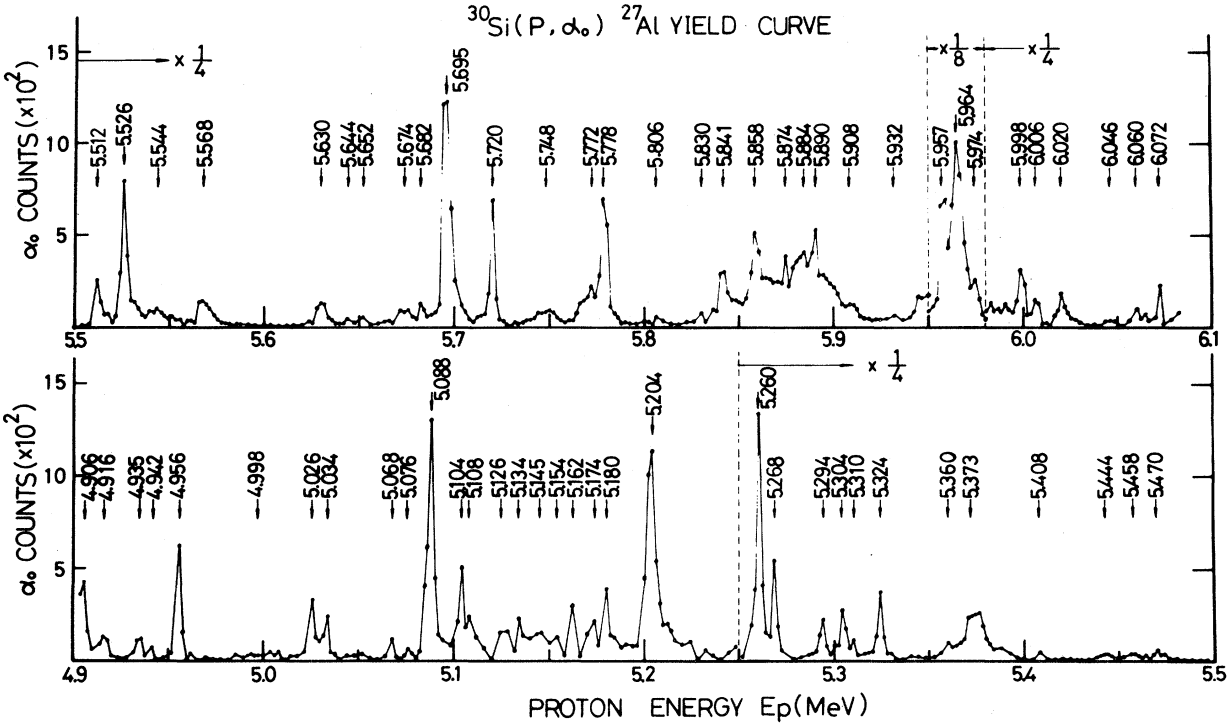

FIG. 3. Excitation function for the ground-state alpha particle produced in the ^{30}Si$(p,\alpha)^{27}$Al reaction. $E_p = 4.900 - 6.082$ MeV. $\theta_\alpha = 120°$ lab. The numbers over the resonance peak indicate resonance energies in MeV.

TABLE I. Resonances in the ^{30}Si(p,α_0) reaction.

E_p (MeV)	E_x (MeV)	Γ (keV)	Yield[a]	Strength (eV)[b] This work	Kuperus[d]
4.906	12.043	<5	51.4	25	18
4.916	12.053	4±2	18.4	8.8	8.6
4.935	12.071	3±2	16.9	8.1	14
4.942	12.078	<4	12.7	6.1	7.7
4.956	12.092	<3	66.4	32	28
4.998	12.125	<20	18.0	8.6	10
5.026	12.159	<4	42.7	21	24
5.043	12.167	<4	24.4	12	28
5.048	12.181	<10	<10.7	<5.1	<3
5.068	12.200	<3	11.9	5.7	10
5.076	12.208	<5	8.11	3.9	<3
5.088	12.219	4±2	169	82	56
5.104	12.235	<4	50.5	24	22
5.108	12.239	<10	43.4	21	
5.126	12.256	8±4	39.4	19	
5.134	12.264	<5	35.5	<17	11
5.145	12.274	<10	35.0	<17	2.7
5.154	12.283	<10	20.6	<10	
5.162	12.291	<6	34.7	17	12
5.174	12.303	<8	37.3	18	19
5.180	12.308	<5	55.7	27	19

TABLE I. (*Continued.*)

E_p (MeV)	E_x (MeV)	Γ (keV)	Yield[a]	Strength (eV)[b] This work	Strength (eV)[b] Kuperus[d]
5.204	12.332	6±3	247	120[c]	120
5.260	12.386	<3	513	251	330
5.268	12.393	<3	205	100	69
5.294	12.419	<5	109	53	53
5.304	12.428	<5	134	66	72
5.310	12.434	<4	34.8	17	24
5.324	12.448	<3	133	66	120
5.335	12.458	<10	19.7	<9.7	<10
5.360	12.482	<8	64.7	32	28
5.373	12.495	12±2	371	228	163
5.388	12.510	<12	<112	<16	12
5.408	12.529	<8	9.23	4.5	7.7
5.444	12.564	<8	30.8	15	
5.458	12.577	<8	38.2	19	
5.470	12.589	<6	36.7	18	
5.512	12.630	<6	123	61	
5.526	12.643	4±2	417	207	
5.544	12.661	<14	127	63	
5.568	12.684	10±3	151	75	
5.630	12.744	8±2	115	58	
5.644	12.757	<6	16.1	8.0	
5.652	12.765	<8	17.0	8.5	
5.674	12.786	<10	91.3	46	
5.682	12.794	<6	52.5	26	
5.695	12.807	6±3	848	424	
5.720	12.831	<3	279	140	
5.748	12.858	12±5	146	73	
5.772	12.881	17±5	368	184	
5.778	12.887	5±3	241	121	
5.806	12.914	<8	32.5	16	
5.830	12.937	<6	47.8	24	
5.841	12.948	4±2	294	148	
5.858	12.964	<8	<431	<216	
5.874	12.980	<6	179	<90	
5.884	12.989	<10	382	<192	
5.890	12.995	<6	325	<164	
5.908	13.013	<8	103	<52	
5.932	13.036	<8	61.9	<31	
5.957	13.060	<4	904	456	
5.964	13.067	8±2	1878	947	
5.974	13.077	<5	24.0	12	
5.998	13.100	5±2	129	65	
6.006	13.107	<6	68.7	35	
6.020	13.121	6±3	120	61	
6.046	13.146	8±4	40.0	20	
6.060	13.160	<10	54.9	28	
6.072	13.171	<3	65.0	33	

[a]Yield obtained by integration of thin target yields at $\theta_{lab} = 120°$ over excitation energy under the resonance peak and expressed in units of alpha particles per 10^{10} incident protons.
[b]Resonance strength $(2J+1)\Gamma_\alpha\Gamma_p/\Gamma$.
[c]Taken from Kuperus (Ref. 12), and used as reference point for the normalization of resonance strengths.
[d]Reference 12.

at the first eight resonances, whose experimental angular distributions are shown in Fig. 4. The ninth resonance at $E_p = 6.020$ MeV exhibits a significant asymmetry around $\theta = 90°$ with strong odd components; this implies that the resonance is affected by levels of different parities. The coefficients from the least-square fit of the data with Legendre polynomials are $A_1 = -0.42 \pm 0.03$, $A_2 = 0.08 \pm 0.06$, $A_3 = 0.08 \pm 0.05$, $A_4 = -0.06 \pm 0.08$, $A_5 = 0.25 \pm 0.06$, and $A_6 = -0.19 \pm 0.09$.

The values of χ^2, calculated from the least-square fit of the experimental distributions with theoretical angular distributions for assumed spin values $\frac{1}{2}$ through $\frac{17}{2}$ at the eight symmetric resonances, are plotted in Fig. 5. Wigner limit reasons restrict J^π values to those shown in the figure. In the cases where χ^2 exceeds the 0.1% probability limit for both parities at a certain J value, only the lowest point has been given.

Table II shows the results from the analysis of the angular distribution measurements at the eight resonances. It presents the Legendre polynomial coefficients of the best one-parameter fit of the observed distribution. Possible solutions for J^π and for the orbital momentum mixing ratio are also given, as well as lower limits for particle widths and dimensionless reduced alpha-particle widths $\theta_\alpha{}^2$. The quality of the measured data for $E_p = 5.512$ and $E_p = 5.998$ MeV resonances has produced one or several J^π values with χ^2 values near the minimum, and therefore these J^π values have been included into possible solutions listed in Table II.

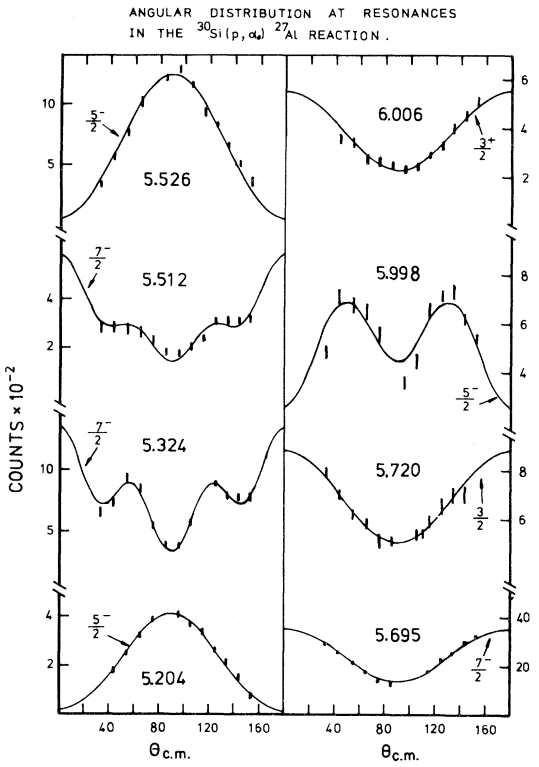

FIG. 4. Angular distributions of the α_0 group from the reaction $^{30}Si(p,\alpha)^{27}Al$ measured at eight resonance bombarding energies. The lines represent the results having minimum χ^2 values from the least-square fits of data points with the one-parameter theoretical angular distributions for the compound nucleus resonance J^π shown near each curve.

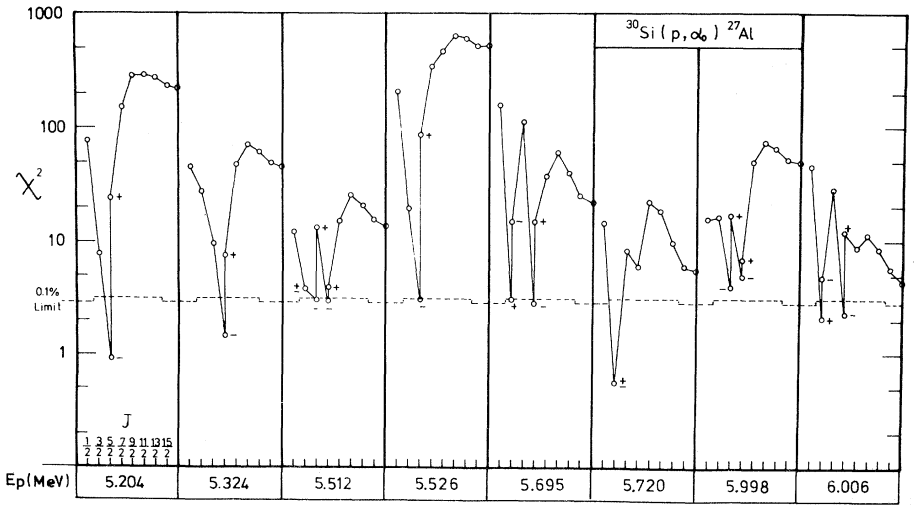

FIG. 5. Angular distribution χ^2 values for different assumed J^π values of the resonance level at eight isolated resonances.

TABLE II. Results from the analysis of angular distributions.

E_p (MeV)	Angular distribution (best one-parameter fit) A_2	A_4	A_6	J^π	Orbital momentum mixing ratios for the possible J values	Γ_{α_0} (eV)	$\theta_{\alpha_0}^2$ $\times 10^2$
5.204	−1.01±0.03	0.08±0.02		$\frac{5}{2}^-$	$(\frac{5}{2}^-)$ −0.12±0.04	≥20	≥0.49[a]
5.324	0.48±0.03	−0.25±0.04	0.67±0.02	$\frac{7}{2}^-$	$(\frac{7}{2}^-)$ 2.8 ±0.3	≥8.3	≥0.22
5.512	0.65±0.02	0.01±0.03	0.53±0.02	$\frac{3}{2}\,\frac{5}{2}^-$ $\frac{7}{2}$	$(\frac{3}{2}^-)$ −1.4 ±0.2 $(\frac{3}{2}^+)$ 1.5 ±0.1 0.26±0.07 −2.7 ±0.3 $(\frac{5}{2}^-)$ 2.7 ±1.4 $(\frac{7}{2}^-)$ 1.5 ±0.1 $(\frac{7}{2}^+)$ 0.6 ±0.1	≥7.6	≥0.073
5.526	−0.96±0.02	0.04±0.01		$\frac{5}{2}^-$	$(\frac{5}{2}^-)$ −0.06±0.02	≥35	≥0.32
5.695	0.69±0.01	−0.04±0.02	0.001±0.001	$\frac{3}{2}^+\frac{7}{2}^-$	$(\frac{3}{2}^+)$ 5.9 ±3.3 $(\frac{7}{2}^-)$ −0.04±0.02 +27(>10, <−6)	≥53	≥0.24
5.720	0.39±0.03			$\frac{3}{2}$	$(\frac{3}{2}^-)$ 1.43±0.13 $(\frac{3}{2}^+)$ 1.46±0.08 0.22±0.04 −2.35±0.16	≥35	≥0.15
5.998	0.01±0.03	−0.55±0.01		$\frac{5}{2}^-\frac{7}{2}^-$	$(\frac{5}{2}^-)$ 1.30±0.14 $(\frac{7}{2}^-)$ −0.95±0.08	≥8.1	≥0.016
6.006	0.65±0.10			$\frac{3}{2}^+\frac{7}{2}^-$	$(\frac{3}{2}^+)$ 3.1 ±0.7 $(\frac{7}{2}^-)$ 0.12±0.10 −6.8 ±3.3	≥4.4	≥0.0087

[a]The corresponding strength has been taken from Kuperus (Ref. 12) and used as the reference point for normalization.

V. DISCUSSION

The experiment investigating resonances in ^{31}P through the ^{30}Si$(p,\alpha)^{27}$Al reaction has several advantages when compared with the experiment through the inverse ^{27}Al$(\alpha,p)^{30}$Si reaction. Despite the requirements of enriched targets and the technique to differentiate alpha particles of low energy and low yield from protons of high energy and much higher yield, the yield of alpha particles in the ^{30}Si$(p,\alpha)^{27}$Al reaction is over a factor of 80 higher than the yield of protons in the inverse reaction when the same resonance in ^{31}P is studied with the same target thickness and the same geometrical conditions. This is due to the fact that thick target yields, $Y^{\max}(\infty)$, have the ratio[17,18,20]

$$\frac{Y_p^{\max}(\infty)}{Y_\alpha^{\max}(\infty)}=\frac{f_p{}^3}{f_\alpha{}^3}\frac{g_\alpha}{g_p}\frac{m_\alpha E_\alpha \epsilon_\alpha}{m_p E_p \epsilon_p}\simeq 8.6\frac{E_\alpha \epsilon_\alpha}{E_p \epsilon_p},$$

where $f=M/(m+M)$, m is the projectile mass, M is the target mass, $g=(2S+1)(2i+1)$, S is the projectile spin, i is the target spin, ϵ is the stopping cross section at projectile energy E, and the subscripts p and α apply to the $p+^{30}$Si channel and the $\alpha+^{27}$Al channel, respectively. The smaller stopping cross sections for the proton beam also make convenient the use of a thin target for the higher excitation region where the density of levels is getting higher. Furthermore, the determination of J^π values of the compound nuclear resonances by the ^{30}Si(p,α) reaction may be greatly simplified if the angular distribution for the alpha particles decaying to the first excited state (E_x=0.844 MeV, $J^\pi=\frac{1}{2}^+$) of ^{27}Al can be measured. In this case both the incoming and the outgoing channels have channel spins $\frac{1}{2}$, which eliminates the possibility of orbital momentum mixing in both channels. The angular distribution for the α_1 group is then completely determined by the spin and parity of the resonance level, in analog to the reaction ^{31}P$(\alpha,p_0)^{34}$S studied by Kuperus.[14] Unfortunately in the present work the α_1 group has not been observed because of very low penetrabilities, and hence this advantage cannot be exploited.

Excitation energies presented in Table I were calculated using the binding energy E_b=7.2968 MeV (Ref. 21) for the $p+^{30}$Si channel, or equivalently E_b=9.6701 MeV (Ref. 21) for the $\alpha+^{27}$Al channel. When these results are compared

with the result of Kuperus,[12] there can be established in the overlapping energy region ($E_x = 12.04 - 12.53$ MeV) a one-to-one correspondence between both measurements, except for a few weak resonances which were clearly observed by Kuperus only through the p_1 group in the ^{27}Al$(\alpha,p)^{30}$Si reaction. However, our excitation energies are generally higher by about 5 keV due to the use of new values of binding energies and possibly of new mass values in this work. In the overlapping region of excitation energy the resonance strengths observed in this work agree, within less than 30%, with those of Kuperus for all resonances except five. It is to be noted that resonance strengths in Kuperus's work were obtained from thick target yields through the reaction ^{27}Al$(\alpha,p)^{30}$Si.

Between $E_x = 12.04$ MeV and $E_x = 13.20$ MeV, 68 resonances have been observed. This corresponds to a mean level spacing of $D = 17.06$ keV, at the mean excitation energy 12.62 MeV. The distribution of the nearest neighbor resonance spacings S, expressed in units of the mean spacing D, is given in Fig. 6 as a histogram. As many different J^π combinations contribute to the observed yield curve, we expect a Poisson distribution[22] $\exp(-S/D')$. The Poisson curve fits well the measured distribution down to $S/D = 0.25$. The dip between $S/D = 0$ and 0.25 is due to the limited resolution of our experiment and indicates that in the investigated energy region about 24 resonances are unresolved or missed. If these missing levels are taken into account, we find an "experimental" level spacing $D' = 12.6$ keV, equivalent to an "experimental" level density $\rho' = 79$ MeV^{-1}. This result will be compared with the semiempirical prediction of Newton.[23] A numerical modification in Newton's expression, as suggested by Preston,[24] was applied, whereas the spin dependence of the average level spacing was

$$D(J^\pi) = D_0(2J+1)^{-1}\exp[J(J+1)/2\sigma^2] ,$$

in which the parameter $2\sigma^2$ was taken from Ref. 25 to be $0.1A^{7/6}E^{1/2}$. Level spacing $D_{\text{pred}} = 8.1$ keV is therefore obtained if one assumes that all resonances populated by $l_p \leq 5$ are detected. However, at $E_x = 12.31$ MeV, the neutron channel opens. Above the neutron threshold, resonances with $J^\pi = \frac{1}{2}^\pm$, $\frac{3}{2}^\pm$, and $\frac{5}{2}^-$ may decay by neutron emission with the lowest allowed $l_n \leq 1$. The corresponding neutron penetrabilities, calculated at $E_x = 12.5$ MeV, are one or two orders of magnitude higher than those probabilities for the case of alpha emission, whose lowest allowed orbital angular momenta are $l_\alpha \geq 1$. Therefore the observation of resonances with $j^\pi = \frac{1}{2}^\pm$, $\frac{3}{2}^\pm$, and $\frac{5}{2}^-$ above neutron threshold is rather unlikely. By performing a calculation where resonances with these J^π values are omitted for excitation energies above neutron threshold, one finds $D_{\text{pred}} = 12.4$ keV, in very good agreement with the experimental value D'. Good agreement of this level density formula with experiments at lower energies has also been shown in Kuperus's work.[12]

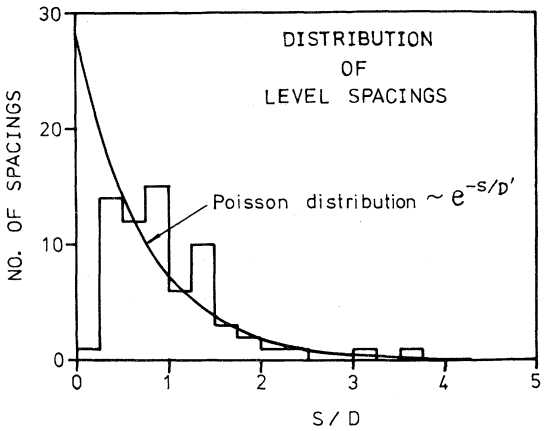

FIG. 6. Histogram of the distribution of the nearest neighbor resonance spacing S. This spacing is given in units of the mean level spacing D. The smooth curve is the Poisson distribution $e^{-S/D'}$.

Angular distributions for two of the levels ($E_p = 5.204$ and 5.324 MeV) investigated in the present experiment have also been observed earlier by Kuperus.[12] Our analysis confirmed their spin and parity assignments ($J^\pi = \frac{5}{2}^-$ and $\frac{7}{2}^-$, respectively). The coefficients of Legendre polynomials and the orbital momentum mixing ratio for the angular distribution at $E_p = 5.204$ MeV level almost completely reproduce Kuperus's result ($A_2 = -1.02 \pm 0.02$, $A_4 = 0.08 \pm 0.02$, and $\varepsilon = -0.13 \pm 0.03$), while those at $E_p = 5.324$ MeV show deviations at A_4 and A_6 coefficients and disagreement at the orbital momentum mixing ratio from Kuperus's result ($A_2 = 0.43 \pm 0.02$, $A_4 = -0.49 \pm 0.03$, $A_6 = 0.116 \pm 0.011$, and $\varepsilon = -0.43 \pm 0.02$).

Based on the previous argument about the neutron emission in competition with alpha emission from resonances above neutron threshold, resonances observed through the ^{30}Si$(p,\alpha_0)^{27}$Al reaction above neutron emission threshold are more likely

to have high spins. From this consideration the ambiguity in the J^π determination from the χ^2 analysis of the angular distribution for a resonance, as shown in Fig. 5, is partially removed. Among the possibilities of J^π for a resonance in Table II, higher spins are favored.

VI. CONCLUSION

We have investigated in the present study the structure of the compound nucleus ^{31}P from the excitation energy 12.04 to 13.20 MeV through the ^{30}Si(p,α)^{27}Al reaction and presented excitation energies, the α_0 strengths and widths for sixty-eight resonances, of which thirty-five are newly reported. The experimental level density is found in good agreement with the result of semiempirical calculation from the formula of Newton[23] and Preston,[24] by taking into account the experimental energy resolution and the neutron emission in competition with alpha emission above neutron threshold. Angular distributions for the α_0 group at nine resonances were analyzed, from which spins and parities were assigned to eight resonance, six of which being reported for the first time. The ninth resonance at E_p=6.020 MeV showed an interference effect due to levels of opposite parities.

This work was supported in part by the National Science Council, Republic of China.

[1]A. C. L. Barnard, S. Bashkin, C. Broude, and C. E. Hornback, Nucl. Phys. 23, 327 (1961).
[2]C. H. Bornman, M. A. Meyer, and D. Reitman, Nucl. Phys. A99, 337 (1967).
[3]C. H. Bornman, M. A. Meyer, N. S. Wolmarans, and D. Reitman, Nucl. Phys. A112, 231 (1968).
[4]H. Willmes and G. I. Harris, Phys. Rev. 162, 1027 (1967).
[5]A. C. Wolff, M. A. Meyer, and P. M. Endt, Nucl. Phys. A102, 332 (1968).
[6]G. Wiechers, W. R. McMurray, and I. J. Van Heerden, Nucl. Phys. A124, 165 (1969).
[7]M. J. A. De Voigt, D. A. Regenboog, J. Grootenhuis, and C. Van der Leun, Nucl. Phys. A176, 97 (1971).
[8]A. K. Val'ter, A. I. Popov, and V. E. Storizhko, Zh. Eksp. Teor. Fiz. 43, 2038 (1962) [Sov. Phys. — JETP 16, 1439 (1963)].
[9]J. Walinga, H. A. Van Rinsvelt, and P. M. Endt, Physica (Utrecht) 32, 954 (1966).
[10]J. Walinga and J. C. H. Oudemans, Physica (Utrecht) 36, 61 (1967).
[11]D. A. Outlaw, G. E. Mitchell, and E. G. Bilpuch, Nucl. Phys. A269, 99 (1976).
[12]J. Kuperus, Physica (Utrecht) 31, 1069 (1965).
[13]L. C. Northcliff and R. F. Schilling, Nucl. Data Tables 7, 233 (1970).
[14]J. Kuperus, Physica (Utrecht) 30, 899 (1964).
[15]J. Kuperus, P. W. M. Glaudemans, and P. M. Endt, Physica (Utrecht) 29, 1281 (1963).
[16]J. Kuperus, Physica (Utrecht) 30, 2253 (1964).
[17]P. B. Lyons, J. W. Toevs, and D. G. Sargood, Nucl. Phys. A130, 1 (1969).
[18]H. E. Gove, in *Nuclear Reactions,* edited by P. M. Endt and M. Demeur (North-Holland, Amsterdam, 1959), Vol. 1, p. 302.
[19]P. R. Bevington, *Data Reduction and Error Analysis for the Physical Sciences* (McGraw-Hill, New York, 1969).
[20]K. A. Snover, Ph.D. thesis, Stanford University, 1969.
[21]P. M. Endt and C. Van der Leun, Nucl. Phys. A310, 1 (1978).
[22]N. Rosenzweig and C. E. Porter, Phys. Rev. 120, 1698 (1960).
[23]T. D. Newton, Can. J. Phys. 34, 804 (1956).
[24]M. A. Preston, *Physics of the Nucleus* (Addison-Wesley, Reading, 1962), p. 527.
[25]J. S. Story, *Nuclear Handbook,* edited by O. R. Frisch (Newnes, London, 1958).